

RESEARCH OUTPUTS / RÉSULTATS DE RECHERCHE

Retrograde Neuroanatomical Tracing of Phrenic Motor Neurons in Mice

Vandeweerd, Jean-Michel; Hontoir, Fanny; De Knoop, Alexis; De Swert, Kathleen; Nicaise, Charles

Published in:

Journal of Visualized Experiments

DOI:

[10.3791/56758](https://doi.org/10.3791/56758)

Publication date:

2018

Document Version

Publisher's PDF, also known as Version of record

[Link to publication](#)

Citation for published version (HARVARD):

Vandeweerd, J-M, Hontoir, F, De Knoop, A, De Swert, K & Nicaise, C 2018, 'Retrograde Neuroanatomical Tracing of Phrenic Motor Neurons in Mice', *Journal of Visualized Experiments*, vol. 2018, no. 132, e56758. <https://doi.org/10.3791/56758>

General rights

Copyright and moral rights for the publications made accessible in the public portal are retained by the authors and/or other copyright owners and it is a condition of accessing publications that users recognise and abide by the legal requirements associated with these rights.

- Users may download and print one copy of any publication from the public portal for the purpose of private study or research.
- You may not further distribute the material or use it for any profit-making activity or commercial gain
- You may freely distribute the URL identifying the publication in the public portal ?

Take down policy

If you believe that this document breaches copyright please contact us providing details, and we will remove access to the work immediately and investigate your claim.

Video Article

Retrograde Neuroanatomical Tracing of Phrenic Motor Neurons in Mice

Jean-Michel Vandeweerdt¹, Fanny Hontoir¹, Alexis De Knoop¹, Kathleen De Swert², Charles Nicaise²

¹URVI, NARILIS, Université de Namur

²URPhyM, NARILIS, Université de Namur

Correspondence to: Charles Nicaise at charles.nicaise@unamur.be

URL: <https://www.jove.com/video/56758>

DOI: [doi:10.3791/56758](https://doi.org/10.3791/56758)

Keywords: Phrenic motor neurons, retrograde labeling, intrapleural, cholera toxin subunit beta, mice, neuroanatomical tracer

Date Published: 9/25/2017

Citation: Vandeweerdt, J.M., Hontoir, F., De Knoop, A., De Swert, K., Nicaise, C. Retrograde Neuroanatomical Tracing of Phrenic Motor Neurons in Mice. *J. Vis. Exp.* (), e56758, doi:10.3791/56758 (2017).

Abstract

Phrenic motor neurons are cervical motor neurons originating from C3 to C6 levels in most mammalian species. Axonal projections converge into phrenic nerves innervating the respiratory diaphragm. In spinal cord slices, phrenic motor neurons cannot be identified from other motor neurons on morphological or biochemical criteria. We provide the description of procedures for visualizing phrenic motor neuron cell bodies in mice, following intrapleural injections of cholera toxin subunit beta (CTB) conjugated to a fluorophore. This fluorescent neuroanatomical tracer has the ability to be caught up at the diaphragm neuromuscular junction, be carried retrogradely along the phrenic axons and reach the phrenic cell bodies. Two methodological approaches of intrapleural CTB delivery are compared: transdiaphragmatic versus transthoracic injections. Both approaches are successful and result in similar number of CTB-labeled phrenic motor neurons. In conclusion, these techniques can be applied to visualize or quantify the phrenic motor neurons in various experimental studies such as those focused on the diaphragm-phrenic circuitry.

Introduction

The aim of the study is to present a reliable method to identify phrenic motor neurons (PhMN) on mouse spinal cord sections. Injection of a fluorescent neuroanatomical tracer in the pleural cavity was chosen as the delivery method to reach the phrenic neuromuscular projections onto the diaphragm and use retrograde transport along the phrenic axons to label phrenic cell bodies. Two techniques of intrapleural delivery are described: transdiaphragmatic versus transthoracic.

Phrenic motor neurons are spinal relay cells whose axons converge into phrenic nerves, which ultimately innervate the diaphragm. These are lower motor neurons receiving the inspiratory drive from the bulbar respiratory centers and relaying it to the diaphragm neuro-muscular junctions (NMJ). PhMN are structured into two motor columns, one for each hemicord, running along the mid-cervical spine. In most of mammalian species including humans, the phrenic motor columns spread from levels C3 to C6^{1,2,3}. We and others have confirmed that PhMN concentrated in C3-C5 levels in rat and mouse spinal cord^{4,5,6,7,8}. The topographical distribution of phrenic cells is not at random; motor neurons innervating the sternal part of the diaphragm are distributed more densely in the cranial part of the phrenic motor pool (C3), whereas motor neurons innervating the crural part are more caudal (C5)⁹. Furthermore, PhMN are clustered variously in the ventral horn gray matter. At C3 level, the clusters of phrenic cells lie laterally, then they shift in a ventrolateral direction and are found ventromedially at the most caudal levels^{10,11}.

Given their vital role during inspiration, it is of the utmost importance to accurately identify PhMN in the healthy spinal cord but also follow their fate during pathological conditions, such as degenerative diseases or traumatic injuries of the spinal cord. Since PhMN do not differ morphologically from other cervical motor neurons, identification of PhMN relies on the targeted delivery of neuroanatomical tracers either at the level of primary respiratory centers⁸, or at the diaphragm NMJ⁷ or in the phrenic nerve⁴. The tracer is taken up by the nerve fibers and carried up to the phrenic cell bodies in the cervical spine, where it can be visualized using direct or indirect detection systems. Retrograde or anterograde tracers are commercially available with a broad range of conjugates. Noteworthy, each tracer is endowed with no, low or high abilities for trans synaptic tracing.

In the current study, we chose the beta subunit of the cholera toxin (CTB) functionalized with Alexa Fluor 555 (henceforth referred to as CTB-fluorophore) as a fluorescent label, allowing a direct visualization of PhMN on frozen spinal cord sections. CTB is usually described as a monosynaptic tracer although experimental data tend to show a transneuronal passage¹². CTB has the ability to bind the ganglioside GM1 at the plasma membrane of the nerve ending. CTB is internalized via clathrin-dependent or -independent mechanisms and traffics through the trans-Golgi network into the endoplasmic reticulum in a retrograde fashion^{13,14}. The internalization and retrograde transport seem to be dependent on the actin cytoskeleton^{15,16} as well as on the microtubule network¹⁷.

To demonstrate the usefulness of CTB as a retrograde neuroanatomical tracer labeling diaphragm-PhMN circuitry, CTB-fluorophore was delivered intrapleurally. CTB was administered using two techniques: the first one included a laparotomy and multiple transdiaphragmatic injections; the second one, less invasive, used a unique transthoracic injection. Four days later, fluorescently-labeled PhMNs were quantified in the cervical spinal cord from both from healthy and from spinally-injured (C4) animals.

Protocol

The experimental protocol was conducted in compliance with the European Communities Council Directives for Animal Experiment (2010/63/EU, 86/609/EEC and 87-848/EEC) and was approved by the Animal Ethics Committee of University of Namur (ethic project n°17-284). **Figure 1** depicts the two respective approaches: transdiaphragmatic or transthoracic injections. Use male C57bl/6J mice (n=18), aged from 3 to 4 months in the study.

1. Preparation of CTB Solution

1. For transdiaphragmatic injections:
 1. Dissolve the CTB powder in sterile water to the concentration of 0.2% (w/v).
 2. Load 7.5 μ L of CTB solution (0.2% w/v) in a sterile 10- μ L-microsyringe with an attached 33-gauge needle (blunt or short bevel) for each mouse.
2. For transthoracic injection:
 1. Dissolve the CTB powder in sterile water to the concentration of 0.1% (w/v).
 2. Load 20 μ L of CTB solution (0.1% w/v) in a sterile 500- μ L-insulin syringe with a beveled 27-gauge needle for each mouse.

NOTE: Make sure to use distilled and sterile water and properly dissolve the CTB powder. The solution can be kept at 4 °C for a month (do not freeze). A precipitate might form after few days. Bring the solution to room temperature and mix well using a pipette before use.

2. Preparation Prior to Intrapleural Injections

1. Sterilize surgical tools prior to surgery, using autoclave or glass-bead sterilizer. Prepare a clean bench coat to do surgery and to dispose the surgical tools.
NOTE: Any material used during the surgical procedure should be sterile. Instruments that cannot be sterilized such as the microsyringe should be wiped down with a disinfectant (chlorhexidine) or should be single-use only. The surgeon should wash her/his hands with a disinfectant (chlorhexidine scrub) before the beginning of the surgery. The surgeon should wear sterile gloves, a facemask, and a clean gown.
2. Weigh animal, and administer an appropriate dose of anesthesia: intraperitoneal injection of anesthetic cocktail (e.g. ketamine 100 mg/kg and xylazine 5 mg/kg).
3. Pinch toe and/or check for the loss of palpebral reflex to determine if the mouse is properly anesthetized. Apply a vet ointment to protect the cornea.
4. Shave carefully the ventral skin (for transdiaphragmatic procedure) or the right-sided thoracic skin (for transthoracic procedure), using electric hair clippers. Shave well and broad enough to prevent hair getting into the surgery field.
5. Ensure aseptic conditions by topical application of 10% iodine solution on the shaved area. Scrub the surgical site with the iodine solution, being careful to scrub from the center of the site toward the periphery.
6. Use a homeothermic pad throughout the surgery to maintain the animal's body temperature.

3. Intrapleural Injections using Transdiaphragmatic Approach

1. Lay down the anesthetized mouse in supine position on a heating pad. Place a rolled gauze pad under the neck of the animal. For an adult mouse, use a rolled gauze pad of 0.5 inch in thickness. Tape this pad to the surgery board to avoid movement if any.
2. Using a scalpel blade, incise the ventral skin along the midline: make an incision from the xiphoid process to the umbilical region while stretching the skin laterally with the other hand to make the skin taut. Do not apply too much pressure on the blade to avoid damaging underlying organs.
3. Using small scissors, carefully detach the skin from the abdominal muscles around the incision. This procedure will help at stitching the muscles and the skin apart at the end of the surgery.
4. Perform laparotomy using small scissors. Open the abdominal cavity by performing a buttonhole incision at the level of the umbilicus. Incise the abdominal muscles along the white line ("linea alba") up to the xiphoid process.
5. In order to visualize the abdominal surface of the diaphragm, retract abdominal muscles using commercial or homemade retractors.
NOTE: These retractors can be made from midi-size paper clips shaped into L-hook¹⁹.
6. Stretch out both sides of the laparotomy, and tape down the retractors to the bench coat. Optimize the illumination of the field of view so that the abdominal surface of the diaphragm is no more in the penumbra. The most powerful lighting device for this purpose is a LED lamp with an orientable light beam.
7. Using soft tweezers in one hand, lift up the xyphoid appendix and pull down the lateral lobes of the liver (**Figure 2A**). Using small scissors in the other hand, carefully cut off the suspensory ligament, without damaging the gallbladder or the diaphragm (**Figure 2B**).
8. Using soft tweezers in one hand, lift up the xyphoid appendix. Grasp the Hamilton syringe in the other hand. Target three sites of injection in the right hemidiaphragm to respectively cover the sternal, the medial and the crural regions (**Figure 3A**, inset in **Figure 3B**).
9. As the diaphragm thickness is around 0.37 mm in mice⁷, insert the needle no more than 1 or 2 mm beyond the diaphragm sheet to prevent lung damages during breathing. Deliver 2.5 μ L of CTB solution (0.2% w/v) through the right diaphragm at each site (**Figure 4B**). Stabilization of the diaphragm is not required.
10. Repeat this procedure for the three ipsilateral sites of injection (**Figure 1A**), and contralaterally for a bilateral labeling of the PhMN pool.
11. To close the laparotomy site, suture abdominal muscles with resorbable 4-0 suture. Use interrupted stitches spaced by 3 mm. Staple skin closed with 9.0 mm wound clips. Tighten staples to prevent animal from pulling off staples. Space staples approximately 5 mm apart. Do not over-tighten the wound clips, as this can lead to impaired healing.

12. Clean micro syringe with distilled water to prevent clogging. Slowly draw up and expel 2-3 times. Do not draw air into syringe.

4. Intrapleural Injection using Transthoracic Approach

NOTE: This method is inspired from the procedure described in rats⁴ and was adapted to mouse.

1. Lay down the anesthetized mouse in left lateral decubitus position, on a heating pad (**Figure 4A**).
2. Identify the sixth and seventh ribs under the elbow region by manual palpation (**Figure 4B**).
3. While an assistant extends right fore- and hind- limbs (**Figure 5A**), insert the syringe cranially oriented and tangentially under the sixth or the seventh rib, 3 mm deep from the skin, with the bevel down (**Figure 1B** and **Figure 5B**).
4. Elevate the needle gently to confirm, by lifting the ribs up, that it is well positioned into the thoracic cavity (**Figure 5C**, insets in **Figure 1B**).
5. Stabilize breathing movements of the chest by applying slight pressure with two fingers on the chest wall.
6. While holding the syringe in the other hand, deliver 20 μ L of CTB solution (0.1% w/v) in a single injection.

5. Post-operative Care

1. Immediately after the procedure, lay the mouse in right lateral decubitus position on a homeothermic pad for recovery. This ensures the tracer to spread on the right side of the pleural cavity and allows for monitoring animal's breathing.
2. Administer 1 mL of sterile saline solution i.p. subcutaneously. Provide follow-up injections if the animal appears dehydrated and/or listless.
3. Administer subcutaneously 0.1 mg/kg of buprenorphine, twice a day during the first two days post-surgery, to minimize any potential pain.
4. Monitor animals daily up to euthanasia.

Representative Results

Male C57bl/6J mice (n=18), aged from 3 to 4 months were included in the study. At day 0 of the experiment, 8 mice underwent a unilateral C4 contusion, right-sided, according to published protocol^{7,18}. As sham procedure, 10 mice underwent a laminectomy on top of C4 without contusion. At day 3, mice were prepared for the intrapleural injections of CTB-fluorophore according to the two different procedures described above. At day 7, all mice were euthanized following anesthesia (ketamine 100 mg/kg and xylazine 5 mg/kg) and exsanguination.

Whole spinal cords were harvested, fixed in paraformaldehyde and cryoprotected in 30% sucrose according to standard lab procedures. Cervical enlargement was isolated, embedded into O.C.T. and cryosectioned longitudinally or transversally at a thickness of 30 μ m.

Longitudinal spinal sections were observed with an epifluorescent microscope equipped with filter cube for fluorescence analysis (Excitation: 560/20nm; Emission: 635/30nm). Fluorescent motor neurons in the ventral horn were identified as a linear column of cells from C3 to C5 levels (**Figure 6A**, upper panel). All labeled cells were located in the ipsilateral gray matter and exhibited morphology consistent with motor neurons (**Figure 6B**). In injured animals, a striking loss of labeled PhMN was observed at C4 level, together with spinal tissue disruption (asterisk in **Figure 6A** and **6C**). CTB⁺ PhMNs were manually counted every fifth transverse section (spaced by 150 μ m) in uninjured and C4-injured spinal cords (**Figure 6C**). An estimation of the total number of labeled PhMNs was calculated by multiplying the number of counted CTB⁺ cells by 5. In uninjured healthy mice, the total number of labeled PhMNs per hemicord was estimated at 151 ± 9 when using transdiaphragmatic (TDia) approach, compared to 178 ± 9 when using transthoracic (TTho) approach (**Figure 6D**). Following C4 injury, these numbers dropped respectively to 59 ± 14 and 70 ± 10 . In this study, no statistical differences were evidenced between the two methods of intrapleural delivery ($p > 0.05$, Mann-Whitney U test; TDia versus TTho).

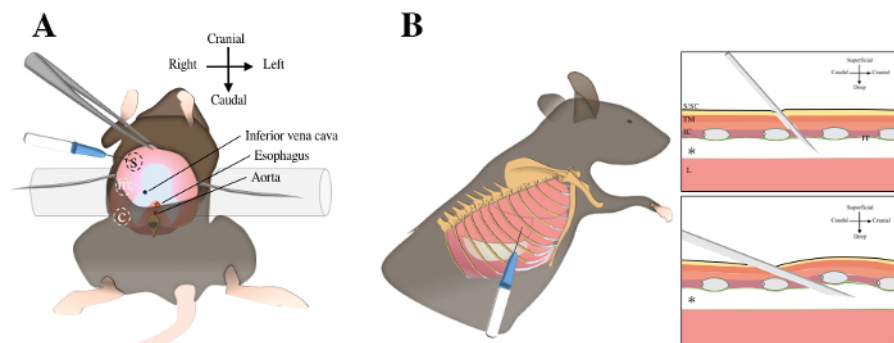


Figure 1. Intrapleural injections using transdiaphragmatic or transthoracic injections. Transdiaphragmatic approach includes a laparotomy, exposure of abdominal surface of the diaphragm (in pink color) and three injections in the sternal, medial and crural regions **A**. For transthoracic approach, the mouse is laid in left lateral decubitus position. The sixth and seventh ribs are identified under the elbow region by manual palpation **B**. The needle is inserted through the skin, the subcutaneous tissue, the thoracic muscles, the intercostal muscles and the parietal pleura to reach the pleural cavity (asterisk). S, sternal; m, medial; c, crural; S/SC, skin and subcutaneous tissue; TM, thoracic muscles; IC, intercostal muscles; pp; parietal pleura; L, lung. [Please click here to view a larger version of this figure.](#)

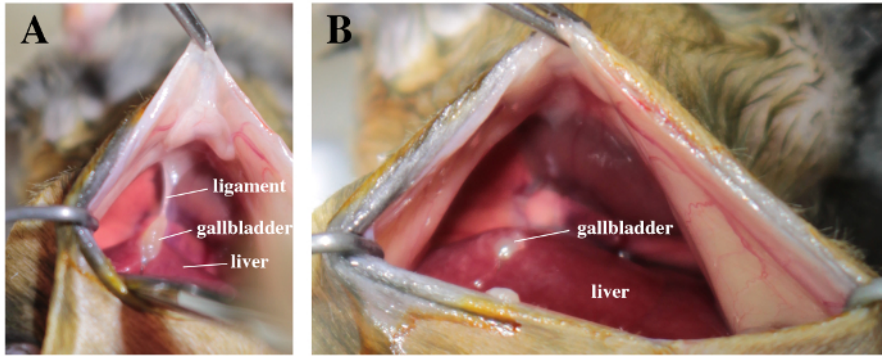


Figure 2. Surgical field with a view on liver, gallbladder and abdominal face of the diaphragm. A. Note the suspensory ligament between the gallbladder and the diaphragm. B. The ligament is carefully cut off. [Please click here to view a larger version of this figure.](#)

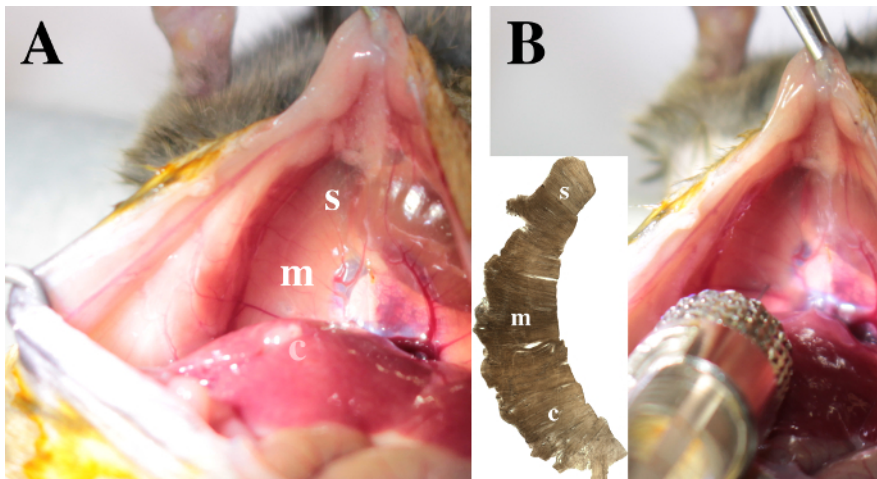


Figure 3. View on the diaphragm. The sternal (s), medial (m) and crural (c) areas are identified in the right hemidiaphragm. A. Note that the crural region is posterior to the liver lobes. B. To inject CTB in the pleural space, insert the needle 1 mm deep through the right hemi-diaphragm. The injection in the medial area is illustrated. [Please click here to view a larger version of this figure.](#)

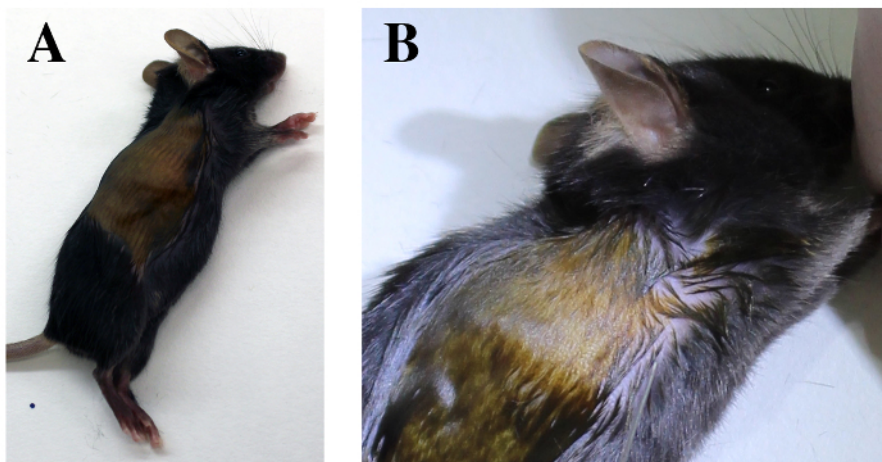


Figure 4. Transthoracic approach. Mouse is positioned in left lateral decubitus A. Identify the costal margin of the diaphragm and the elbow region. B. The sixth and seventh intercostal spaces are identified deep to the elbow region. [Please click here to view a larger version of this figure.](#)

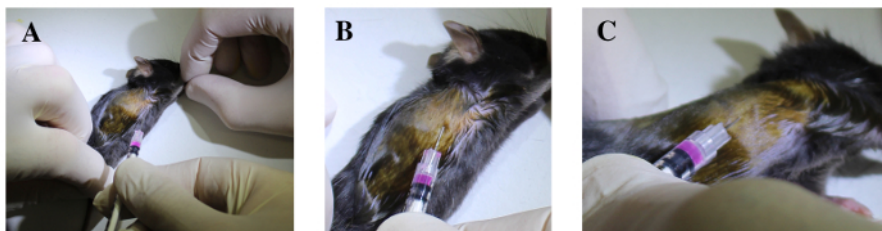


Figure 5. The sixth and seventh intercostal spaces are identified deep to the elbow region. A. Fore- and hind- limbs are extended. **B.** The syringe is cranially oriented and tangentially inserted under the sixth or the seventh rib, 3 mm deep through the intercostal muscles, with the bevel upside-down. **C.** The needle is gently elevated and the ribs are lifted to confirm the needle is well positioned into the thoracic cavity. [Please click here to view a larger version of this figure.](#)

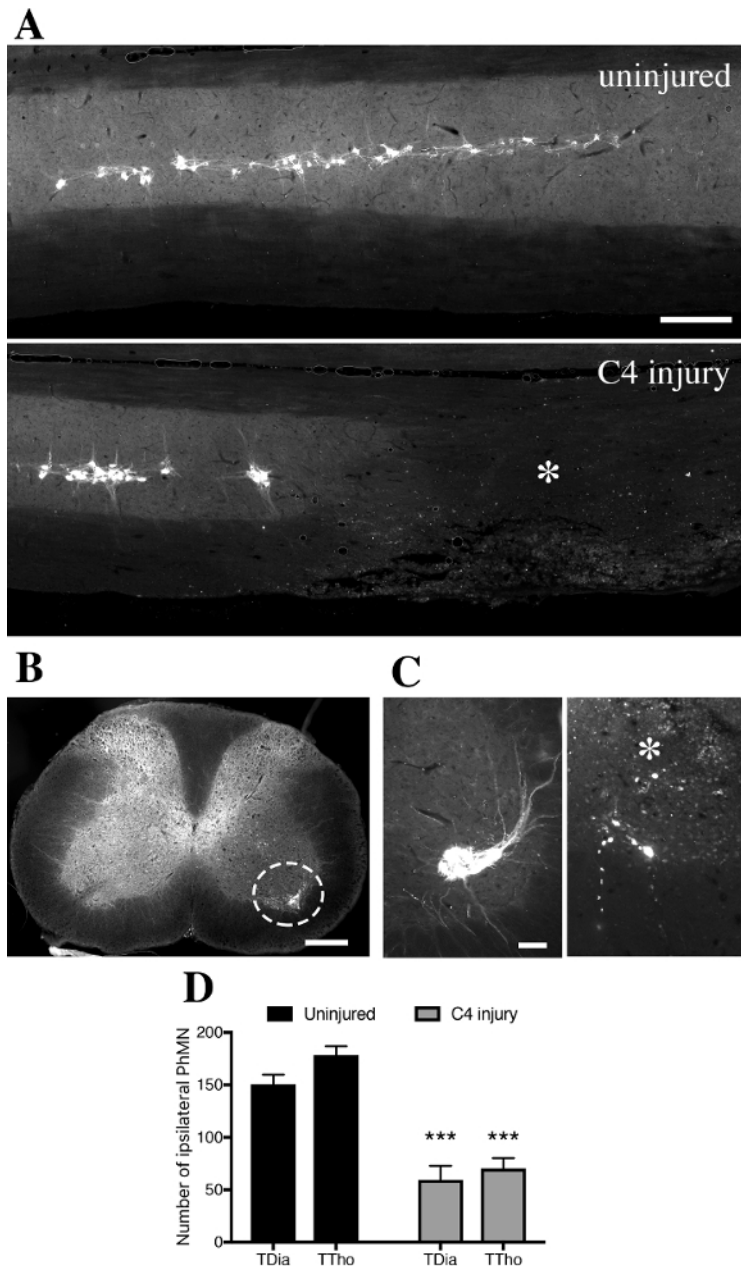


Figure 6. CTB⁺ cells in the ventral horn gray matter of intrapleurally-injected mice. **A.** In spinally-uninjured mouse, CTB⁺ phrenic motor neurons distribute along the cervical spinal cord from level C3 to C5. In contused mouse, tissue disruption is observed unilaterally with loss of CTB⁺ phrenic motor neurons at C4 level (asterisk). **B.** Labeled CTB⁺ cells were located in the ipsilateral gray matter and exhibited morphology consistent with motor neurons. **C.** Transverse sections of spinal cords were used to quantify the number of CTB⁺ cells at specific distances along the spinal cord in uninjured (left) and injured (right) mice. **D.** Quantification of CTB⁺ cells found in the ipsilateral hemicord in uninjured or injured mice, according to the transdiaphragmatic (TDia) or transthoracic (TTho) approach of intrapleural CTB delivery. Bars represent 250 μ m. Data were expressed as the mean \pm standard error of the mean (SEM). n= 5-7 mice in each TDia group; n= 3 mice in each TTho group. Non-parametrical Mann-Whitney U tests were performed and results were considered as significantly different for p<0.05. ***p<0.001 for uninjured versus C4 injury. [Please click here to view a larger version of this figure.](#)

Discussion

The protocol described herein can be applied to any strain of adult mice or to any experimental paradigm in which the integrity of the diaphragm-PhMN circuitry should be evaluated. For instance, amyotrophic lateral sclerosis (ALS) and cervical spinal cord injury (cSCI) are conditions associated with PhMN loss, anterograde degeneration of phrenic axons and subsequent respiratory compromise. Animal models of ALS or cSCI mimic histopathological and functional respiratory deficits observed in human diseases. In these models, histological techniques are often applied to evaluate PhMN survival following various therapeutic interventions aiming at PhMN neuroprotection^{18,20,21}. Any trouble of uptake at the

diaphragm NMJ or axonal transport will undoubtedly compromise the amount of CTB accumulated in the neuronal cell bodies. Loss of phrenic axons or PhMN degeneration will obviously decrease the amount of CTB retrotransported into the spinal cord.

Each approach of intrapleural administration has its own pros and cons. Transdiaphragmatic injections are quite invasive, necessitating laparotomy and careful stitching of all skin layers to prevent dehiscence and organ protrusion. Laparotomy interferes with normal respiration²² and one cannot rule out that it may affect PhMN activity or retro-transport efficiency. However, the direct visualization of the diaphragm during the injection ensures successful targeting of the pleural space all the time. Transthoracic injections are minimally-invasive compared to transdiaphragmatic injections and can thus be considered as a procedure for Refinement, in the vein of "Three Rs" concept. One drawback is the increased likelihood of being off-target for an inexperienced user (e.g. in the subcutaneous tissue or in the chest wall).

Following intrapleural fluorescent-CTB administration, it is likely that any motor neuron projecting onto muscles lining the pleural cavity will be labeled, including PhMN, intercostal motor neurons or different populations of brainstem motor neurons. In adult rats, Mantilla et al. demonstrated that intercostal motor neurons were also labeled in the ventral horn of thoracic spinal cord, as well as some dorsal root ganglion neurons⁴. We have never checked the presence of CTB-labeled cells in other sites than the cervical spinal cord in mice.

Depending on the experimental settings/models, outcome measures can include the columnar arrangement of PhMNs along the cervical spinal cord, detailed analysis of geometrical data about the position of each PhMN or, as described here, the quantification of PhMN number. The accurate evaluation of total PhMN number depends on technical considerations and inter-evaluator reliability; because of the variability of CTB fluorescence intensity, neuron soma size or background staining. In our experience using transdiaphragmatic injections of CTB-fluorophore, we have estimated the number of PhMN per mouse hemisection in a range between 120 and 180 cells, a number of a bit less than data from other groups⁸. Indeed, there are two limitations of the study. First, a limited number of animals are injected using the transthoracic approach and second there is an uncertainty on complete labeling of PhMN pool. Phrenic nerve dip (after nerve transection) or intraneural injections with fluorescent neuroanatomical tracer are complementary techniques that can be used to more accurately label all PhMNs. For future studies, it is recommended to count PhMNs by unbiased methods such as stereology.

In our experience, we have never observed any obvious respiratory deficit or complications (respiratory distress) such as bleeding or pneumothorax following this procedure. However, if the diaphragm has been damaged during the transdiaphragmatic injections, consider using a needle of smaller diameter or with sharper bevel.

To avoid animal death during or after surgery carefully check the concentrations of each component in the anesthetic cocktail. Avoid making injuries onto the surfaces of the liver, the intestine, the gallbladder or the diaphragm.

No or low labeling of PhMN could be due to several issues. If the transthoracic injection misses the pleural cavity, re-do and check by manual palpation that the needle is inserted under the ribs or do not pop out through the skin. No bubbles should form upon injection of CTB solution. Remember also that that the internalization of CTB in the nervous cell is pH-dependent²³: acidic and neutral pH are optimal while basic pH impairs the uptake of the toxin. It is recommended to resuspend CTB powder in water, in saline or in PBS buffer. Consider the persistence time of the labeled toxin in the neuronal cell body. In our experience, we could detect CTB-labeled cells in a time window between four days and two weeks after intrapleural delivery. Decreasing the time allocated to retrograde transport or increasing the time between intrapleural delivery and sacrifice might compromise the optimal detection of fluorescent-CTB in the tissue.

To avoid fluorescence fading use proper fixative method. We suggest perfusing the animal's body with buffered 4% paraformaldehyde. Once the spinal cord is harvested, incubate in the same fixative overnight. Cryoprotect the cord in sucrose 30% solution for 72 hours until sinking, then embed the cervical enlargement (about 8 mm) in O.C.T. medium. Do not dehydrate or embed the sample in paraffin. Protect spinal samples or tissue sections from light during the whole post-processing. Fixed whole spinal cords can be kept at 4 °C for months if thimerosal is added to the cryoprotectant solution (do not add sodium azide as it will provoke fluorescence fading). Tissue sections can be kept at -20 °C for months away from light. Finally, we advise to mount the slides with an anti-fading reagent. If the fluorescence has faded, it is still possible to detect CTB using immunohistochemistry.

Disclosures

The authors have nothing to disclose.

Acknowledgements

We are grateful to Robert Graffin and Pauline Duhant for their technical support.

References

1. Webber, C. L., Jr., Wurster, R. D., & Chung, J. M. Cat phrenic nucleus architecture as revealed by horseradish peroxidase mapping. *Exp Brain Res.* **35** (3), 395-406 (1979).
2. Goshgarian, H. G., & Rafols, J. A. The phrenic nucleus of the albino rat: a correlative HRP and Golgi study. *J Comp Neurol.* **201** (3), 441-456 (1981).
3. Gordon, D. C., & Richmond, F. J. Topography in the phrenic motoneuron nucleus demonstrated by retrograde multiple-labelling techniques. *J Comp Neurol.* **292** (3), 424-434 (1990).
4. Mantilla, C. B., Zhan, W. Z., & Sieck, G. C. Retrograde labeling of phrenic motoneurons by intrapleural injection. *J Neurosci Methods.* **182** (2), 244-249 (2009).
5. Nicaise, C. et al. Early phrenic motor neuron loss and transient respiratory abnormalities after unilateral cervical spinal cord contusion. *J Neurotrauma.* **30** (12), 1092-1099 (2013).

6. Nicaise, C. et al. Phrenic motor neuron degeneration compromises phrenic axonal circuitry and diaphragm activity in a unilateral cervical contusion model of spinal cord injury. *Exp Neurol.* **235** (2), 539-552 (2012).
7. Nicaise, C. et al. Degeneration of phrenic motor neurons induces long-term diaphragm deficits following mid-cervical spinal contusion in mice. *J Neurotrauma.* **29** (18), 2748-2760 (2012).
8. Qiu, K., Lane, M. A., Lee, K. Z., Reier, P. J., & Fuller, D. D. The phrenic motor nucleus in the adult mouse. *Exp Neurol.* **226** (1), 254-258 (2010).
9. Laskowski, M. B., & Sanes, J. R. Topographic mapping of motor pools onto skeletal muscles. *J Neurosci.* **7** (1), 252-260 (1987).
10. Feldman, J. L., Loewy, A. D., & Speck, D. F. Projections from the ventral respiratory group to phrenic and intercostal motoneurons in cat: an autoradiographic study. *J Neurosci.* **5** (8), 1993-2000 (1985).
11. Gottschall, J. The diaphragm of the rat and its innervation. Muscle fiber composition; perikarya and axons of efferent and afferent neurons. *Anat Embryol (Berl).* **161** (4), 405-417 (1981).
12. Lai, B. Q. et al. Cholera Toxin B Subunit Shows Transneuronal Tracing after Injection in an Injured Sciatic Nerve. *PLoS One.* **10** (12), e0144030 (2015).
13. Torgersen, M. L., Skretting, G., van Deurs, B., & Sandvig, K. Internalization of cholera toxin by different endocytic mechanisms. *J Cell Sci.* **114** (Pt 20), 3737-3747 (2001).
14. Chinnapen, D. J., Chinnapen, H., Saslowsky, D., & Lencer, W. I. Rafting with cholera toxin: endocytosis and trafficking from plasma membrane to ER. *FEMS Microbiol Lett.* **266** (2), 129-137 (2007).
15. Fujinaga, Y. et al. Gangliosides that associate with lipid rafts mediate transport of cholera and related toxins from the plasma membrane to endoplasmic reticulum. *Mol Biol Cell.* **14** (12), 4783-4793 (2003).
16. Badizadegan, K., Wheeler, H. E., Fujinaga, Y., & Lencer, W. I. Trafficking of cholera toxin-ganglioside GM1 complex into Golgi and induction of toxicity depend on actin cytoskeleton. *Am J Physiol Cell Physiol.* **287** (5), C1453-1462 (2004).
17. Abbott, C. J. et al. Imaging axonal transport in the rat visual pathway. *Biomed Opt Express.* **4** (2), 364-386 (2013).
18. Li, K. et al. Overexpression of the astrocyte glutamate transporter GLT1 exacerbates phrenic motor neuron degeneration, diaphragm compromise, and forelimb motor dysfunction following cervical contusion spinal cord injury. *J Neurosci.* **34** (22), 7622-7638 (2014).
19. Lepore, A. C. Intraspinal cell transplantation for targeting cervical ventral horn in amyotrophic lateral sclerosis and traumatic spinal cord injury. *J Vis Exp.* (55) (2011).
20. Llado, J. et al. Degeneration of respiratory motor neurons in the SOD1 G93A transgenic rat model of ALS. *Neurobiol Dis.* **21** (1), 110-118 (2006).
21. Lepore, A. C. et al. Focal transplantation-based astrocyte replacement is neuroprotective in a model of motor neuron disease. *Nat Neurosci.* **11** (11), 1294-1301 (2008).
22. Sieck, G. C., & Fournier, M. Diaphragm motor unit recruitment during ventilatory and nonventilatory behaviors. *J Appl Physiol* (1985). **66** (6), 2539-2545 (1989).
23. Janicot, M., Clot, J. P., & Desbuquois, B. Interactions of cholera toxin with isolated hepatocytes. Effects of low pH, chloroquine and monensin on toxin internalization, processing and action. *Biochem J.* **253** (3), 735-743 (1988).